Journal of Pharmaceutical and Biomedical Analysis 192 (2021) 113649

Contents lists available at ScienceDirect

Journal of Pharmaceutical and Biomedical Analysis

journal homepage: www.elsevier.com/locate/jpba

An SPRi-based biosensor pilot study: Analysis of multiple circulating extracellular vesicles and hippocampal volume in Alzheimer's disease

Silvia Picciolini, Alice Gualerzi, Cristiano Carlomagno, Monia Cabinio, Stefano Sorrentino, Francesca Baglio, Marzia Bedoni*

IRCCS Fondazione Don Carlo Gnocchi, Via Capecelatro 66, Milan, Italy

ARTICLE INFO

Article history:
Received 14 June 2020
Received in revised form
10 September 2020
Accepted 15 September 2020
Available online 23 September 2020

Keywords:
Extracellular vesicles
Surface plasmon resonance imaging
Biosensor
Alzheimer's disease
Hippocampal volume

ABSTRACT

One of the main hurdles in the study of Alzheimer's Disease (AD) is the lack of easily accessible and sensitive biomarkers for the diagnosis, the prediction of the disease progression rate and the evaluation of rehabilitative and pharmacological treatments. Extracellular Vesicles (EVs) are nanoscale particles released by body cells, studied as promising biomarkers of AD as they are involved in the onset and progression of the disease. In the strive for a reliable and sensitive method to analyze EVs, we applied our recently developed biosensor based on Surface Plasmon Resonance imaging (SPRi) technology for the identification and profiling of neural EVs populations circulating in the plasma of 10 AD patients and 10 healthy subjects. The SPRi-array was designed to separate simultaneously EVs released by neurons, astrocytes, microglia and oligodendrocytes, and to evaluate the presence and the relative amount of specific surface molecules related to pathological processes including translocator protein (TSPO), β-Amyloid and ganglioside M1.

As results, significant variations in the relative amount and cargoes of specific brain-derived populations of EVs were observed comparing EVs coming from AD patients and healthy subjects, finding the main differences in the activation phenotype of microglia EVs, in the lipid moieties on generic EVs and in the β-Amyloid expression on surfaces of neuronal EVs.

Besides, the demonstrated correlation of SPRi data with Magnetic Resonance Imaging analysis, provided support for using the SPRi-based biosensor for the evaluation of neurodegeneration detecting and characterizing circulating EVs as peripheral biomarkers for the diagnosis and monitoring of progression and rehabilitation treatments in AD patients.

1. Introduction

Alzheimer's Disease (AD) is a progressive neurodegenerative disorder manifesting with progressive decline in cognitive functions and accompanied by deterioration in emotional control, social behavior or motivation. AD is the most common form of dementia in the elderly (>65 years old), affecting nearly 35 million people worldwide and this number is expected to triple by 2050 due to the increase of lifespan, thus making AD a public health priority [1]. In its typical clinical form, AD manifestations start with memory decline associated with the neurodegeneration in medial temporal lobe structures (i.e. hippocampus) and progress towards a more global cognitive decline, paralleled by diffuse brain atrophy involving higher-order and associative cortices. In 2011 with National Institute on Aging and Alzheimer's Association (NIA-AA) guidelines [2], AD became a clinical-biological entity where biomarkers were used to support the diagnosis of AD symptomatic subjects, to identify preclinical AD-condition from a biological point of view, and to improve the possibility to monitor the disease progression and the responsiveness to therapeutic and rehabilitative treatments. Currently, AD biomarkers are classified in the ATN system [3]: biomarkers of β-amyloid deposition (A), pathologic tau (T), and neurodegeneration (N). In the ATN framework the diagnosis of AD refers to a biological construct and the umbrella term of *"Alzheimer's continuum"* is adopted to describe clinical-biological disease across AD phases [4]. A and T biomarkers obtained from the cerebrospinal fluid (CSF) and/or imaging (PET) are available with good diagnostic value, but they lack the power to predict disease progression as

Abbreviations: AD, Alzheimer's disease; HC, healthy control; EVs, extracellular vesicles; SPRi, Surface Plasmon Resonance imaging; TSPO, translocator protein; GM1, ganglioside M1; Aβ, amyloid-β peptide; MRI, magnetic resonance imaging; CSF, cerebrospinal fluid; MoCA, Montreal Cognitive Assessment.

* Corresponding author at: Laboratory of Nanomedicine and Clinical, BiophotonicsIRCCS Fondazione Don Carlo Gnocchi, Via Capecelatro 66, 20148, Milano, Italy.
E-mail address: mbedoni@dongnocchi.it (M. Bedoni).

https://doi.org/10.1016/j.jpba.2020.113649
0731-7085/

they reach their maximum change at the initial stage of the pathology [5]. Besides, the invasive collection of CSF and the high costs of PET imaging limit their use in the clinical practice and a number of blood-based biomarkers to be added in the ATN system are currently under investigation for AD. Plasma levels of Aβ, protein Tau and neurofilament (NfL), and β secretase 1 (BACE) activity are the main blood-based biomarkers in development for AD; other proteins, microRNAs, amino acids and lipids have also demonstrated positive predictive value with the need of further validation studies [6]. Nonetheless, the extremely low concentration of brain-derived molecules in blood, together with the complexity of the matrix, hamper the development of blood AD biomarkers, suggesting the need for a multiplexing analysis of definite sets of biomarkers and for the development of innovative platforms that can improve the analytical accuracy. In this scenario, Extracellular Vesicles (EVs) are emerging valuable candidate biomarkers for AD [7]. EVs are secreted membrane vesicles characterized by nanoscale dimensions bounded by a lipid bi-layer that hosts both membrane-bound and transmembrane proteins, while the vesicle lumen is filled with cytosolic proteins as well as nucleic acids. EVs coming from neural cells are present in CSF and also in the blood. Although the mechanism by which EVs cross the blood-brain barrier is not well understood, multiple evidence suggests that, in cases of disease and inflammation processes, the damage or breakdown of the barrier allows the transfer of EVs from the brain into the periphery [8]. EVs complex cargo of multiple bioactive and pathological molecules, both proteins and nucleic acids, can mirror the status and the biochemical features of the brain. It has been reported that the cargo of neural EVs reflects the typical hallmarks of AD, mainly related to neuroinflammation and synaptic dysfunction [9], but also plasma vesicles derived from astrocytes were demonstrated to be implicated in the pathogenic mechanisms of AD, thus demonstrating their potentiality as complex vehicles for AD biomarkers [8].

The detection and the quantification of multiple EV populations and their pathological antigens need a reliable and sensitive method that can overcome the current technical limitations, mainly due to their heterogeneity, nanoscale dimensions and amount, that make difficult the validation of EVs as biomarkers [10]. It is worth noting that detecting brain-derived EVs in blood plasma is challenging because they represent a small fraction of the whole circulating EVs. In the strive for a reliable and sensitive method to analyze EVs, we were inspired by the remarkable development of plasmonic biosensors having the ability to detect nanovesicles derived from biological samples [11]. In particular, Surface Plasmon Resonance imaging (SPRi) is a label-free and sensitive analytical technique able to monitor in real-time, variations in the mass adsorbed on the surface of a gold layer, allowing to simultaneously detect multiple molecules within 200 nm from the surface. As this range closely matches the EVs size, SPRi has been validated as an effective method for the profiling of EVs membrane proteins [12,13].

In the present work, we aimed to identify the populations of EVs most involved in AD and to evaluate the presence and relative amount of markers related to neuroinflammation and Aβ plaques formation, by using an SPRi-based biosensor that we have designed and previously tested for human EVs analysis [13]. Moreover, to detect the relationship between the proprieties of circulating neural EVs (i.e. the amount of specific molecules involved in AD pathogenesis) with the level of severity of the disease, we correlated the biochemical content of circulating neural EVs with hippocampal volume as a biomarker of neuronal injury and global cognitive level as an index of cognitive impairment. Our results suggest that the amount of specific neural populations of EVs and the specific cargo of each identified EV population could be candidated as a novel diagnostic and prognostic tool that may become available in the future. The developed biosensor platform could potentially lead to the accurate and reliable diagnosis managing the AD symptoms in a personalized way at its onset, the monitoring of the disease progression, the early treatment of patients, the evaluation of the efficacy of new therapeutics and rehabilitation protocols and to the enhancement of the clinical trials performances.

Table 1
General characteristics of the subjects enrolled in the study.

Parameters	AD	HC	p-values
Number	10	10	–
Males/females ratio	4/6	5/5	0.0661
Age (mean ± std dev)	73.9 ± 3.0	62.6 ± 2.0	0.0002
MoCA (mean ± std dev)	20 ± 2.4	–	–
Total hippocampal volume mm^3 (mean ± std dev)	4534.47 ± 353.17	–	–

2. Materials and methods

2.1. Patients recruitment and peripheral blood sample collection

10 AD patients were recruited at Memory Clinic IRCCS S. Maria Nascente of Fondazione Don Carlo Gnocchi (FDG; Milan, IT). All participants or their representatives provided informed written consent, following the protocol approved by the Ethical Committee of Fondazione Don Carlo Gnocchi, according to the declaration of Helsinki. Inclusion criteria for AD were considered: diagnosis of AD according to NIA-AA criteria [2]; mild dementia stage as documented with a Clinical and Dementia Rating (CDR) scale score between 0.5 and 1; absence of psychiatric or systemic illness. To have a global index of cognitive functioning, all subjects performed cognitive evaluation using the Montreal Cognitive Assessment test (MoCA). Demographic features are reported in Table 1.

Peripheral blood samples (10 mL) were collected from each patient. To avoid the variability due to the clot formation, blood samples were collected using EDTA-treated tubes (BD Vacutainer, Becton Dickinson), centrifuged first at 1300 *g* (10 min) and then at 1800 *g* (10 min) to isolate the plasma, obtaining about 3 mL for each subject. Plasma samples were coded, anonymized and frozen at −80 °C divided into aliquots.

2.2. Isolation and characterization of extracellular vesicles

EVs were isolated from the blood plasma of AD patients and of an additional group of 10 Healthy subjects (HC), for the comparison between patients and non-pathological controls. Inclusion criteria of HC were considered: age ≥ 60 years, no history of dementia, absence of psychiatric or systemic illness (demographic features are reported in Table 1). The Table shows that subjects are matched for gender but not for age; AD patients are older than HC subjects. This age differentiation makes the analysis a pilot study with the aim to verify the feasibility of the analysis of circulating EVs as biomarkers through SPRi technology.

We have submitted all relevant data of our EVs isolation and characterization experiments to the EV-TRACK knowledgebase (EV-TRACK ID: EV200062) [14]. EVs isolation was performed by Size Exclusion Chromatography (SEC) using qEV original columns (Izon Science, Christchurch, NZ) as previously described [13]. Briefly, 500 μL of centrifuged plasma was loaded on top of a column and fractions from 7 to 11, containing EVs, were collected, stored at −20 °C in PBS with protease inhibitor cocktail (Merck) until use.

Isolated EVs were characterized for their protein content, morphology, size distribution and concentration. Total protein content of EV samples was measured by BCA assay (Pierce BCA assay kit, Thermo Scientific, Waltham, MA, USA). To confirm the presence of vesicles with typical morphology and size range, 5 μl of freshly isolated EVs were incubated on Formvar carbon-coated grids, stained with 2% uranyl acetate solution for 10 min and dried. Transmis-

sion electron microscope images were obtained with Leo 812AB (Zeiss, Oberkochen, DE) operating at 80 kV. Nanoparticle Tracking Analysis (NTA) was performed using NanoSight NS300 Instrument (Malvern) with flow-cell top-plate, in order to evaluate the size distribution and the concentration of isolated EVs. The NTA analysis was performed on a random subsample of 3 subjects for each group (AD and HC). EVs were diluted in filtered PBS and recordings of the movements of particles were collected for 60 s, three times for each sample.

2.3. SPRi EVs analysis

Once isolated and characterized as described in paragraph 2.2, EV samples were analyzed by SPRi. The SPRi analysis required 3 steps: the preparation of SPRi biochip; the detection of multiple EV populations coming from distinct cells in the plasma; the analysis of expression levels of specific markers on each identified EV population.

2.3.1. Preparation of SPRi biochip

An array of antibodies/lectin was conjugated on top of SPRi gold chips by using an SPRi-arrayer (Horiba Scientific SAS, Palaiseau, FR), following the previously published protocol [13]. Briefly, after the cleaning of the gold surface using piranha solution, the chip was coated with a Self-Assembled Monolayer (SAM) of thiolated PEG molecules (TH 001-m11.n2 and TH 003-m11.n6; ProChimia Surfaces, Sopot, PL) for the conjugation of ligands on the chip, using EDC/NHS chemistry in order to capture EVs as close as possible to the gold surface. The spotting procedure for the ligands immobilization (0.5 μg/mL) was performed at room temperature with a metal-ceramic capillary pin of 0.7 mm spot diameter for direct contact spotting procedure. The families of ligands spotted on a chip for the microarray preparation are the following: Anti-CD171 (14-1719-82, eBioscience, Inc, San Diego, CA, USA), Anti-CD9 (14-0098, eBioscience), Anti-EphrinB (HBM-EPH-50, HansaBioMed, Tallinn, EE), Anti-PLP1 (HBM-PLP-50, HansaBioMed), Anti-IgG (407402, BioLegend Inc, San Diego, CA, USA), Anti-CD81 (MAB 4615, R&D Systems, Minneapolis, MN, USA), Anti-Glast (EAAT1/GLAST-1/SLC1A3 Antibody, NB100-1869SS, Novus Biologicals LLC, Centennial, CO, USA), isolectin B4 (IB4) from *Bandeiraea simplicifolia* (L3019, Merck), anti-CD11b (553311, BD Biosciences, San Jose, CA, USA). The chip was then blocked in a solution of ethanolamine (1 M, pH 9) for 30 min, washed with water and stored at 4 °C with a layer of StabilCoat Immunoassay stabilizer (Sigma-Aldrich) for the preservation of the activity, until use.

2.3.2. SPRi detection of multiple of EV populations

SPRi measurements were performed using XelPleX instrument (Horiba Scientific SAS, Palaiseau, FR). Every experiment was anticipated by accurate instrument calibration with the injection of 200 μl of sucrose (3 mg/mL) at 50 μl/min flow rate. Experiments were performed using HBS-ET as running buffer (1.5 M NaCl, 100 mM HEPES, 30 mM EDTA, Tween 0.5 %, pH 7.4). 500 μl of EVs samples (20 μg/mL of total protein content) were injected in the SPRi flow chamber with a flow rate of 25 μl/min in order to isolate the EVs populations coming from neurons (CD171/EphrinB), oligodendrocytes (PLP1), astrocytes (Glast), microglia/macrophages (IB4, CD11b) according to the interaction between their specific antigens and the ligands spotted on the SPRi chip. This analysis provided quantitative information on the relative amount of EVs coming from distinct brain cells in the plasma.

2.3.3. SPRi analysis of expression levels of specific membrane EV markers

The surface of the immobilized EVs was further analyzed to evaluate the expression of other specific markers on each identified EV population. In particular, the molecules used for the characterization of each EV subpopulation are: PK-11195 (C0424, Merck), Anti-β 6E10 (Purified anti-β-Amyloid, 1–16 Antibody, 803001, BioLegend) and Anti-Ganglioside GM1 (ab23943, Abcam plc, Cambridge, UK). To this aim, 200 μl of 200 nM solution of the secondary analyte (PK-11195, Anti-β 6E10 and Anti-GM1) was consecutively injected on the SPRi chip at 25 μl/min. Glycine (50 mM, pH 2, 200 μl at 50 μl/min) was used for the regeneration of the chip between the analyses.

2.4. Quantification of β-amyloid monomers in plasma

Plasma levels of monomers of beta amyloid 40 (Aβ40), the most prominent peptide, and beta amyloid 42 (Aβ42), the most neurotoxic form, were quantitated with enzyme-linked immunosorbent-type assays using the High Sensitivity Human Amyloid β40 and Amyloid β42 ELISA (EZHS-SET, Merck) according to the manufacturer's instructions. The selected ELISA kit can reliably detect even low levels of Aβ peptides (detection limit 6 pg/mL) using monoclonal anti-Aβ antibodies with high selectivity for human Aβ. Each sample was analyzed in duplicate and the Aβ42/40 ratio, which has been reported as a better indicator of the AD pathology, was calculated. Mann-Whitney non-parametric test was used to compare data obtained from AD and HC samples.

2.5. MRI data acquisition and data analysis

All AD subjects underwent a single MRI examination on a 1.5 T Siemens scanner (Magnetom Avanto) including conventional sequences to exclude brain abnormalities and a high-resolution 3D-T1 image to perform hippocampal volumetric measurements (TR =1900 ms; TE =3.37 ms; TI =1100 ms; flip angle = 15°; 176 contiguous, 1 mm isometric voxel; FOV = 192 mm × 256 mm).

Cortical reconstruction and volumetric segmentation (including the computation of the estimated Total Intracranial Volume) of 3D-T1 images were performed with the Freesurfer image analysis suite, which is documented and freely available for download online (http://surfer.nmr.mgh.harvard.edu/). Manual quality check was performed according to ENIGMA pipeline (http://enigma.ini.usc.edu/protocols/imaging-protocols). Total hippocampal volume (left + right) was computed according to Iglesias et al. [15] and was considered as a biomarker of neuronal injury. Total hippocampal volume was included in subsequent statistical correlation analyses in association with SPRi data.

2.6. Data analysis and correlation analysis

SPRi data were analyzed using EzSuite (Horiba) and Origin2018 (OriginLab, Northampton, MA, USA) software. For each experiment, the SPRi signal collected on anti-IgG spots was used as negative control and subtracted to the signals obtained on the other ligands spotted on the same chip. Then, signals related to the EV injection were normalized for the mean intensity of Anti-CD9 spots present on the same chip, as CD9 is a marker of generic EVs, not specific for a particular cell of origin. This allowed us to overcome eventual artifacts related to the EV isolation step and to compare data from multiple experiments and multiple samples. For the subsequent characterization of EV populations immobilized on the chip, the SPRi signals of the secondary analytes (PK-11195, Anti-β 6E10 and Anti-GM1) were normalized for the amount of EVs detected on each family of ligands, making possible a more precise profiling of EV populations, as already proposed and verified by our previous work [13].

Statistical analysis was performed using Origin2018. Mann-Whitney non-parametric test was used to compare data obtained from the EV characterization. Pearson's correlation index was used

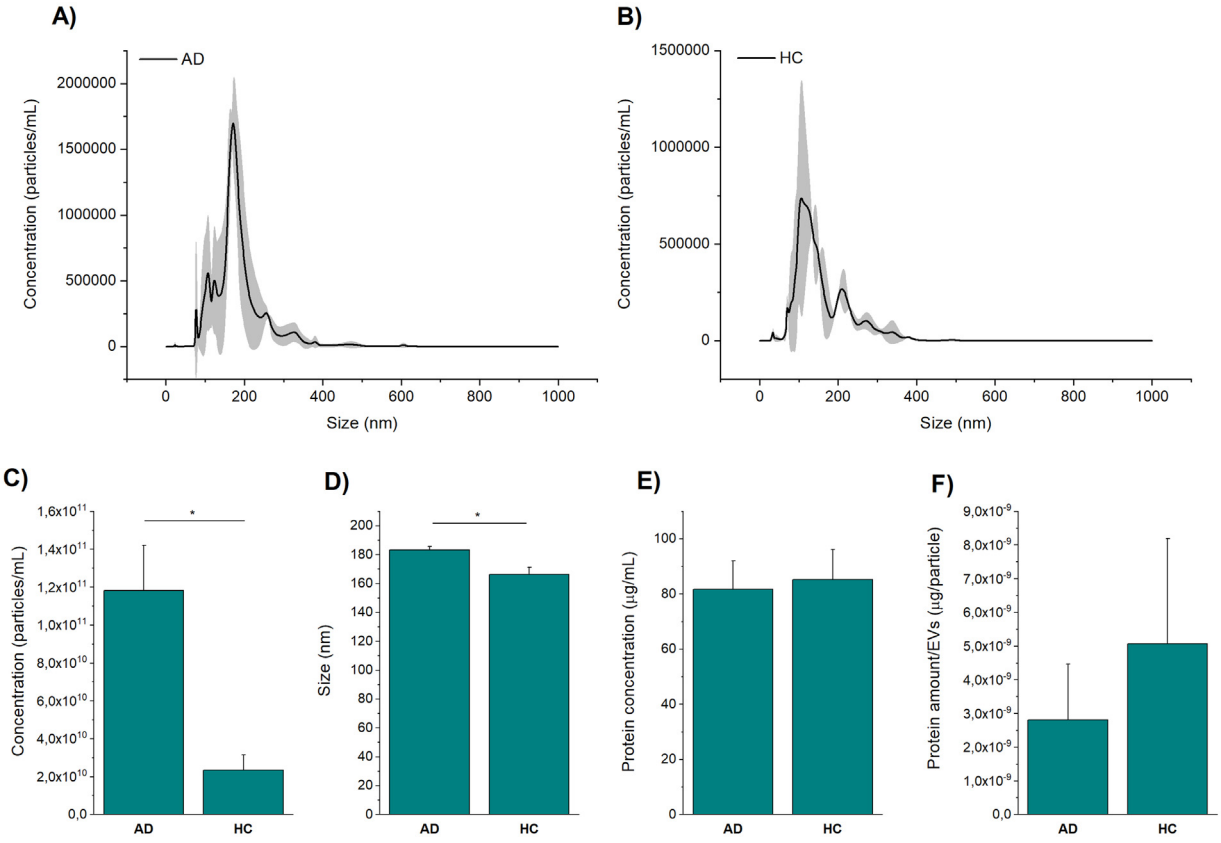

Fig. 1. EVs characterization: **A-B)** NTA analysis of EVs. Average (black line) and standard deviation (grey band) related to the dimensional dispersion of 3 EV samples from AD patients (A; diluted 1:1000 in filtered PBS) and HC subjects (B; diluted 1:500 in filtered PBS); **C)** Concentration of EVs in plasma samples obtained by NTA. Non parametric Mann–Whitney test demonstrated that the means of the AD and HC groups are significantly different ($p < 0.05$); **D)** The mean size of AD and HC EV samples obtained by NTA. The means are significantly different ($p < 0.05$, Mann–Whitney test); **E)** Protein concentration in EV samples from AD and HC subjects measured by BCA assay ($p > 0.05$, Mann–Whitney test); **F)** Amount of total protein per EVs isolated from HC and AD subjects ($p > 0.05$, Mann–Whitney test).

to assess the linear correlation between the SPRi data (CD11b/IB4) and the age of AD and HC subjects. Moreover, the partial correlations were performed between SPRi data (regarding the relative amounts of EV populations) and total hippocampal volume, collected from AD subjects, covariated for intracranial volume. The index was identified as statistically relevant for p-values < 0.05.

3. Results and discussion

3.1. Extracellular vesicles characterization

EVs from blood plasma of AD patients and HC were successfully isolated by SEC and characterized following the ISEV guidelines MISEV2018 [16]. In particular, particle number and size were measured by NTA finding a higher concentration of EVs in AD patients ($1.18*10^{11}$ particles/mL) than in HC subjects ($2.34*10^{10}$ particles/mL) (Fig. 1A, B and C), with a mean size of 183 ± 4.6 nm for AD group and of 167 ± 9.4 nm for HC (Fig. 1D). The Mann–Whitney test performed on the NTA data demonstrated that the EV concentration and size of AD and HC subjects are significantly different ($p = 0.0286$). Moreover, the values related to the total protein content obtained by BCA assay, showed that the disease does not significantly affect the total protein content present in EVs (Fig. 1E, $p = 0.8534$ Mann–Whitney test); however, the protein amount per EVs (µg/particles) appeared to be reduced in AD patients compared with HC, with no significant difference (Fig. 1F). Despite the small sample size, these data are in accordance with trends previously demonstrated and published by Perrotte M. et al. [17]. The characterization by TEM confirmed that the isolated particles owed the typical EV size range and cup-shaped morphology (Fig. 2). Finally, the protein content calculated through the BCA assay data was used to determine the volume of each EV sample to be injected on the SPRi chip.

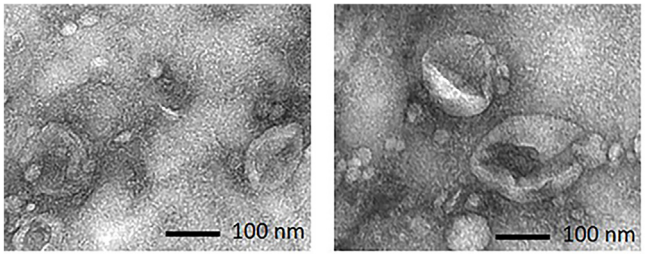

Fig. 2. TEM images of EVs isolated from human plasma of subjects involved in the study. Scale bar 100 nm.

3.2. Multiple detection of circulating extracellular vesicles

To study the differences in the amount and composition of the EVs present in the plasma of AD patients and HC subjects, we took advantage of our previously optimized SPRi-based biosensor that allows the specific detection and characterization of multiple subpopulations of EVs [13]. As circulating EVs include also the brain-derived ones, we designed the SPRi microarray for the simultaneous detection of vesicles coming specifically from neurons, astrocytes, oligodendrocytes and microglia, according to the presence of typical membrane molecules, following the protocol

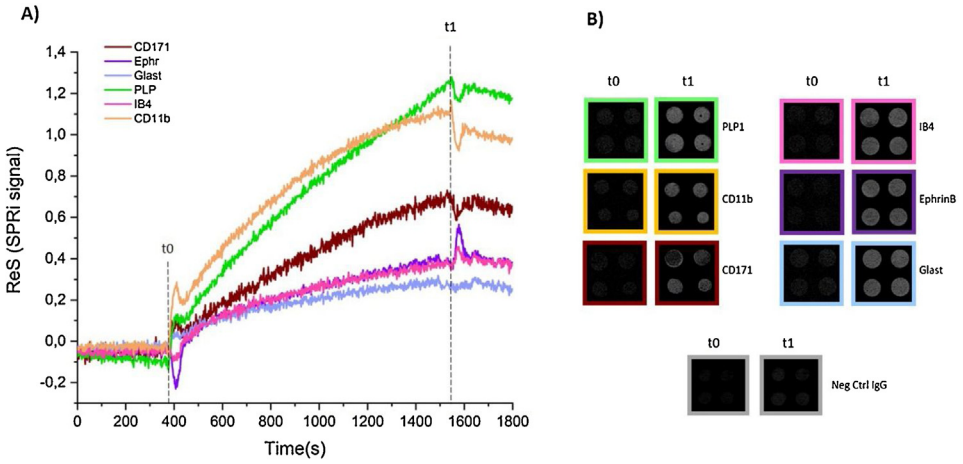

Fig. 3. A) SPRi sensorgram related to the injection of 500 μL of EVs (20 μg/mL) on a chip with an array of 7 families of ligands (4 spots of each family). Each curve is the average of the signal collected on the 4 spots of the same ligand. t0 indicates the time when the injection of the sample starts, and t1 when it ends. Each signal is the subtraction between the signal obtained on the specific ligand family and the signal obtained on the Negative ctrl family (IgG) spotted on the same chip. **B)** CCD differential images without any subtraction (reflectivity variation) of each spot on the SPRi chip acquired at t0 and t1.

described in section *2.3.2 of Material and Methods*. In particular, CD171 and EphrinB were used as neuronal EV markers [18,19], Glast as a marker of astrocytes-derived EVs [20], PLP1 as marker of oligodendrocytes-derived EVs [21], IB4 and CD11b as a markers of vesicles secreted from non-activated and activated microglia, respectively [22,23]. Once EVs were injected on the biosensor, the signals were collected in correspondence of the spots where the above cited ligands (antibodies or lectin) were attached on the chip surface, thus confirming the ability of the SPRi-platform to detect plasma EVs from multiple cell sources. Fig. 3A shows the sensorgram related to the injection of one EV sample on the prepared microarray. The graph makes apparent the multiplexing ability of the SPRi platform to identify simultaneously each EV family. Indeed, each signal is related to the interaction between the ligand spotted on the chip and the corresponding analyte; the intensities of SPRi signals at the end of EVs injection are indicative of the amount of EVs that effectively interact with each spotted ligand. Fig. 3B shows the raw images (no subtraction performed) of the spots before and after the sample injection making visible the effective immobilization of vesicles occurring during the experiment. Actually, the XelPlex SPRi instrument allows the real-time imaging of the chip, where the mass adsorbed on each spot can be visualized on a video CCD camera: the high-resolution CCD video provides real-time difference images capturing all of the local changes occurring at the chip surface. Therefore, we have verified the suitability and the efficacy of the optimized SPRi platform for the specific, sensitive and multiple detection of circulating EVs released by different cell types, including astrocytes, neurons, microglia and oligodendrocytes; according to these results we decided to use this platform to perform the comparative study of EVs in AD patients and HC.

3.3. Brain-derived extracellular vesicles populations in plasma of AD and HC subjects

The circulating EV from AD and HC subjects were analyzed with the SPRi platform, injecting for each subject 500 μL of EV samples with 20 μg/mL of total protein content measured by BCA assay. Thanks to the proportional relationship between SPRi signal and the analyte adsorbed on each spot, the obtained data provide an overall representation of the relative amount of different neural EV populations that circulate in the blood of each considered subject. In general, the comparison between patients and controls showed a significant increase in brain-derived EVs in AD patients. The statistical analysis (Mann-Whitney test) performed on these data showed a significant difference (p-value < 0.05) between the two groups for EphrinB+ (p = 0.0164), Glast+ (p = 0.0448), PLP1+ (p = 0.0216) and IB4+ (p = 0.0069) EVs (Fig. 4A). These data suggest that in AD there is an imbalance of EV release, causing an increase in the amount of brain-derived vesicles in the plasma, in particular EVs coming from neurons, astrocytes, oligodendrocytes and microglia. This observation supports the hypothesis that the inflammatory and pathological process occurring in AD induce modifications in the blood-brain-barrier that might allow an easier transfer of vesicles from the brain to the blood [8]. Besides, the increased amount of circulating brain-derived EVs constitutes an advantage in terms of biomarker analysis, because it allows a better identification and characterization of their cargoes and promotes the feasibility of the study of the circulating EVs as markers of pathological events occurring in the brain. In particular, the variation in the relative amount of specific brain-derived populations of EVs can represent a first indication of the status of the brain by mirroring ongoing pathological processes.

Moreover, considering the important contribution of neuroinflammation to the AD pathogenesis [4] and the possible involvement of EVs in pathological processes, we focused our attention on the microglia-derived EVs data. As shown in Fig. 4B, slight variations in the activated phenotype of the microglia cells releasing EVs were observed: the higher ratio observed in AD patients between SPRi signal intensity of activated (CD11b+) and non-activated microglia EVs (IB4+) revealed that there is an increase in the neuroinflammation-associated EVs in plasma of AD patients compared to HC, being indicative of a neuroinflammatory status. Although neuroinflammation cannot be considered an exclusive hallmark of AD, our data are in agreement with the plethora of data underlying the crucial role of microglia during AD pathogenesis [24]. Then, we verified whether the increased CD11b/IB4 ratio could be due to physiological ageing as brain microglia could be dysregulated with age causing chronic neuroinflammation, but no correlation was found between the neuroinflammation index and age for all considered subjects (p-value = 0.18948 – Pearson's test).

3.4. Relationship between EV populations amount and MRI data

In patients with AD, we found a significant partial correlation (p = 0.031) between the values of the CD11b/IB4 ratio and the total hippocampal volume, considering the total intracranial volume as

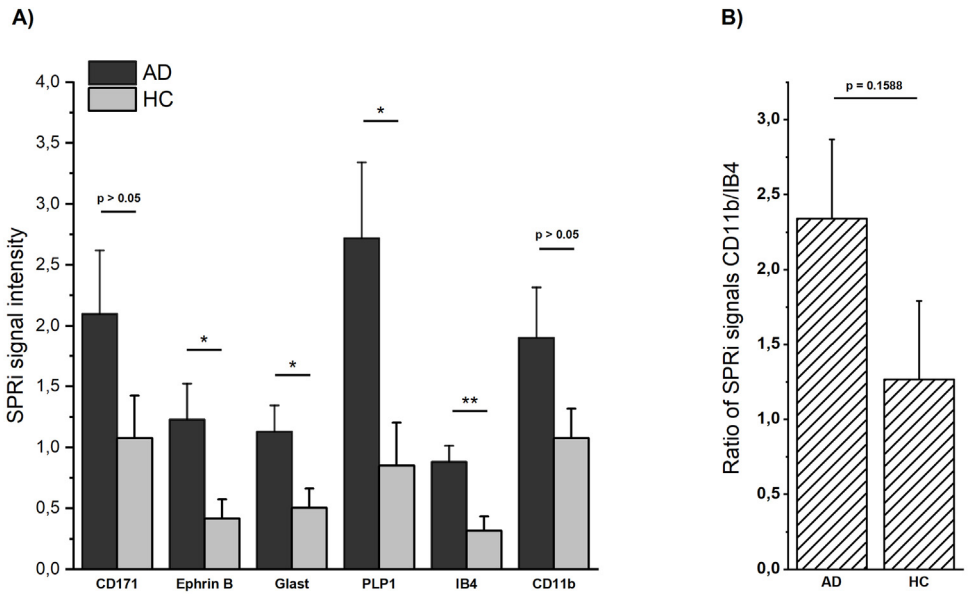

Fig. 4. A) SPRi intensities (average and standard error) related to the injection of EVs of 10 AD patients and 10 HC subjects. The signals are normalized for the intensities collected on a Anti-CD9 family spotted in parallel on each SPRi chip. P-values of Mann-Whitney test: CD171, p = 0.1588; EphrinB, p = 0.0164; Glast, p = 0.0448; PLP1, p = 0.0216; IB4, p = 0.0069; CD11b, p = 0.0535. **B)** Average and standard error of the ratio between the SPRi signals obtained on Anti-CD11b and IB4 spots for the AD and HC group of subjects.

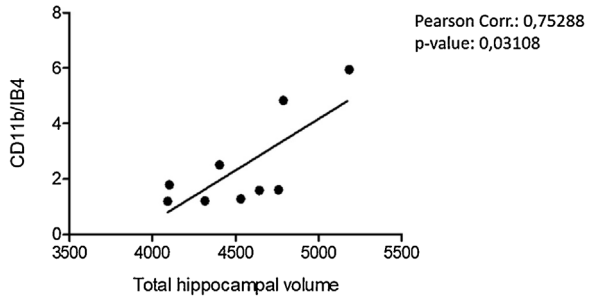

Fig. 5. Scatterplot related to the correlation between CD11b/IB4 ratio and the total hippocampal volume obtained through MRI test for the selected AD patients. The partial correlation coefficient and relative p-value of the correlation, corrected for total intracranial volume, are 0.75288 and 0.03108, respectively.

covariate (Fig. 5). This finding suggests a relationship between the value of the CD11b/IB4 ratio and the severity of neurodegeneration further supporting the literature data about the role of inflammatory processes in neurodegeneration [25]. Although the differences observed in the amount of the other EV populations between AD and HC subjects (Fig. 4A), we didn't observe other significant or relevant correlations between the MRI data and the amount of the brain-derived EV populations.

3.5. Levels of specific molecules on different brain-derived EVs populations from AD and HC subjects

The main strength of the herein developed biosensor is its potentiality to be used not only for the simultaneous detection of different EV populations, but also for their concomitant characterization in terms of levels/presence of other specific membrane molecules of interest. As the EVs are studied as carriers of AD biomarkers, the surface of each vesicle population was characterized. We investigated the presence and relative amount of specific molecular components potentially involved in those processes known to occur during the disease progression. In this context, we decided to focus on the expression of translocator protein (TSPO), amyloid beta peptide (Aβ) and ganglioside M1 (GM1) molecules on the different immobilized EVs populations from both AD and HC. After the EV injection, we introduced in sequence a high affinity ligand of TSPO (PK-11195), the Anti-β-Amyloid antibody and the Anti-GM1 antibody.

3.5.1. Analysis of TSPO on EVs

TSPO, also known as peripheral benzodiazepine receptor (PBR), is an 18 kDa protein present on the mitochondria of activated microglia, astroglia and macrophages. The expression levels of TSPO are associated with neuroinflammation, thus identifying TSPO as a biomarker of inflammatory conditions occurring in AD, stroke, Parkinson's disease, brain injury and other diseases [26]. The SPRi signals related to PK-11195 injection were normalized for the amount of immobilized EVs and demonstrated the presence of TSPO on the membrane of vesicles from neurons, microglia, astrocytes and oligodendrocytes, as well as on CD9+ vesicles of undefined cell source. Our data showed a higher expression of TSPO on generic EVs (CD9+) in AD patients compared to control samples (p = 0.0530 – Mann-Whitney test) (Fig. 6A). Looking at the brain-derived populations, TSPO was more abundant on neuronal and microglia derived EVs (CD171+ and IB4+) in AD patients than in HC (SPRi signal intensity on CD171+ in AD: 1.61, in HC 0.78; SPRi signal intensity on IB4+ in AD: 0.89, in HC: 0.32). Whereas, astrocytes and oligodendrocytes derived EVs (Glast+ and PLP1+) did not show a difference in TSPO expression between the two groups (Fig. 6B). These data, together with the previous observation about the increased CD11b/IB4 ratio, suggest that the neural EV populations mainly involved in the neuroinflammatory processes occurring in AD are those derived from microglia and neurons.

3.5.2. Analysis of β-amyloid and GM1 on EVs

It is well known that GM1 accumulated on the cell surfaces is involved in the aggregation mechanisms of Aβ leading to the deposition of plaques behind the process of neural degeneration that causes the neuronal and synaptic dysfunction. Besides, it was reported that GM1 presence on the surfaces of EVs can contribute to extracellular amyloid fibril formation [27], and that Aβ peptide levels in plasma EVs are higher in AD patients compared to HC subjects

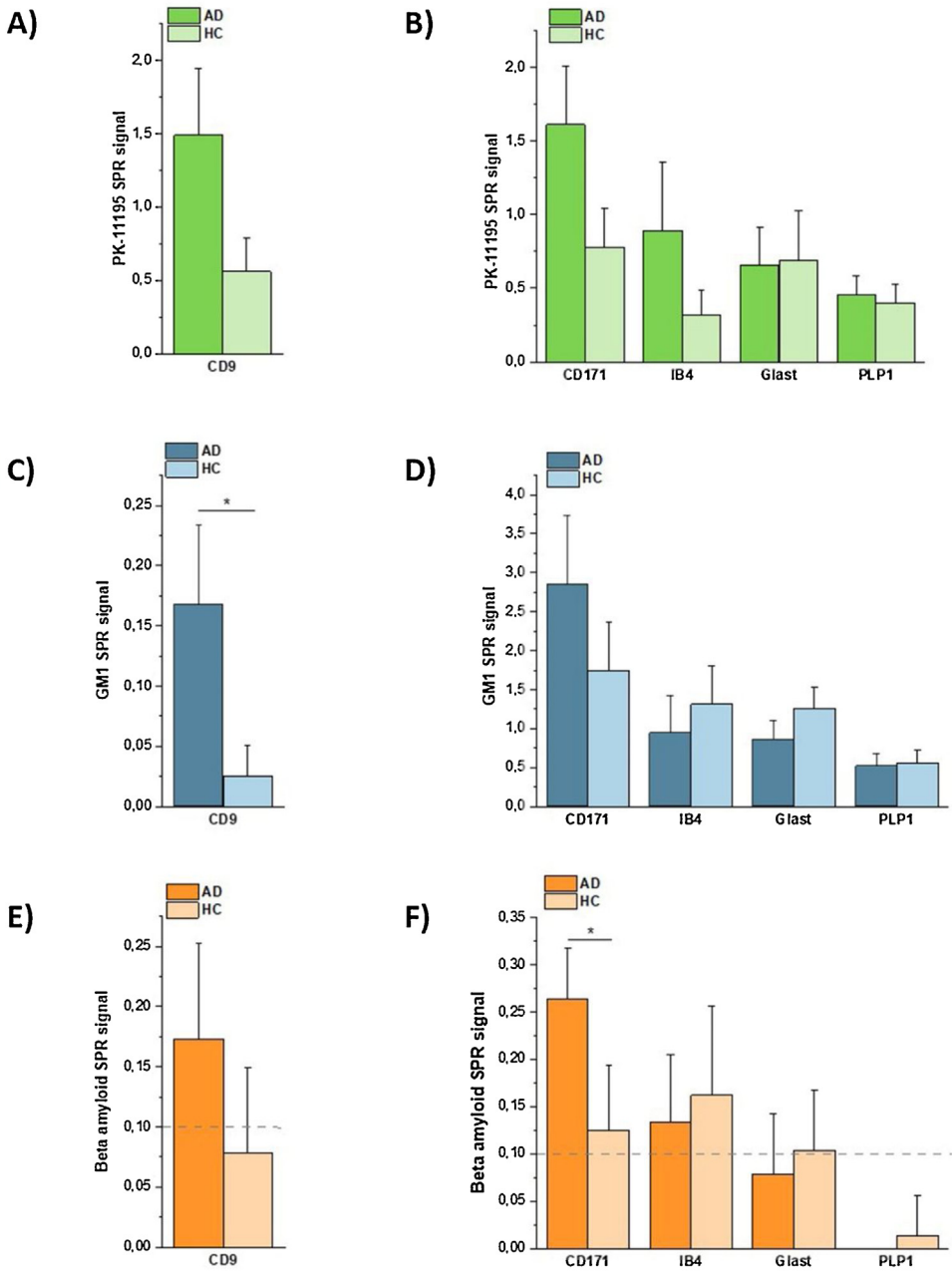

Fig. 6. SPRi intensities (average and standard error) related to the injection of 200 μL of PK-11195 (A-B), Anti-GM1 (C-D) and Anti-β-amyloid (E-F)——— after the EVs for 10 AD patients and 10 HC subjects. The signals are normalized for the amount of EVs previously immobilized on each spot. Dashed lines indicate the level under which the signal intensity is negligible (<0.1). In Figure C the signals are statistically different between the 2 groups (p = 0.0298, Mann-Whitney test). In Figure F the signals on CD171+ EVs are statistically different between AD and HC (p = 0.0464, Mann-Whitney test).

[28]. Still, those EV subtypes directly involved in the GM1-amyloid aggregation process have not been identified, yet.

The herein developed SPRi-based biosensor allowed the evaluation of the presence of GM1 on the surface of the selected circulating EV populations. In particular, the injection of Anti-GM1 antibody on the EVs immobilized on the chip has revealed that GM1 is significantly more abundant on CD9+ EV membranes in AD patients than in HC subjects (p = 0.0298 – Mann-Whitney test) (Fig. 6C). The differences in the lipid moieties were also observed on neuronal-derived EVs (CD171+ EVs) with an increment of GM1 in AD patients, while the other neural EV populations didn't show a significant difference between the 2 investigated groups (Fig. 6D). These data suggest the involvement of neuronal EV population in the GM1-related mechanisms, in agreement with previously reported data [27].

In parallel, in the same experiment, the SPRi analysis of Aβ peptide on EVs revealed to us that AD patients present relevant levels of Aβ peptide on plasma EVs, whereas these levels are negligible in HC (signal intensity < 0.1) (Fig. 6E). Moreover, the study on different EV populations showed that Aβ peptide i) is not present on astrocytes and oligodendrocytes-derived EVs, ii) is present in low amount on IB4+ EVs without differences between AD and HC and iii) is present on the membranes of CD171+ EVs only of AD patients (Fig. 6F). These data provide a direct evidence that a significant amount of Aβ peptides are associated with the external surface of brain derived vesicles that circulate in plasma, especially of neuronal origin. Although we cannot totally exclude a partial rupture of some EVs in our samples and thus the possible release of amyloids from the EV lumen before the injection, the significant increment of

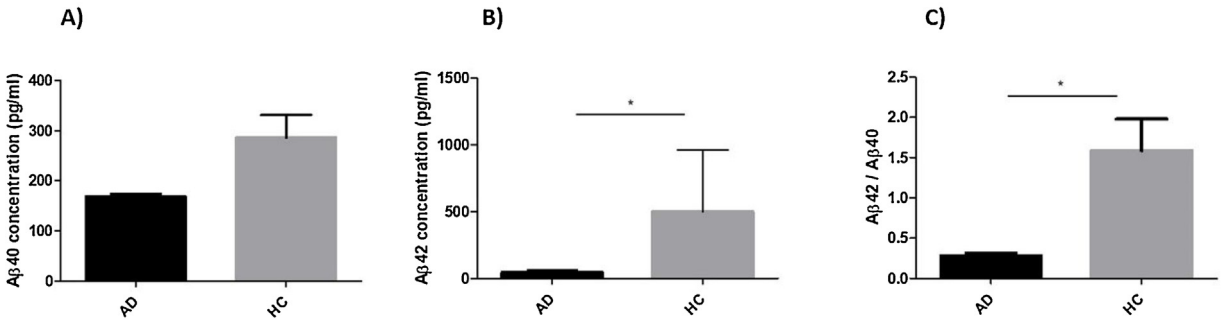

Fig. 7. Quantification of β-amyloid in plasma samples. **A)** Average and standard error of plasma levels of Aβ40 in AD and HC samples; **B)** Average and standard error of plasma levels of Aβ42 in AD and HC samples; **C)** Ratio of the plasmatic concentrations of Aβ42 and Aβ40 in AD and HC subjects.

binding of the Anti-β-Amyloid antibody provides clear evidence of the presence of Aβ peptides on the vesicle surface, a much debated topic. Taking together the data on GM1 and Aβ expression levels on neural EVs, it seems that circulating CD171+ EVs are carriers of both these markers, which could play a connected role in the mechanism of amyloid fibril formation.

3.6. Plasma levels of β-amyloid

Plasma levels of Aβ40 and Aβ42 were measured on AD and HC samples using the ELISA assay. Their expression was found reduced in AD (Aβ40: AD 168 pg/mL, HC 286 pg/mL; Aβ42: AD 47 pg/mL, HC 501 pg/mL), with the Aβ40/Aβ42 ratio lower in AD patients than in HC ($p = 0.0288$ – Mann-Whitney test) (Fig. 7). Similar trends have been observed in recent studies, which described the Aβ clearance decrease from the AD brain and the association of Aβ40/Aβ42 ratio with a decline of attention, memory and executive functioning, reporting that it could be used for diagnosis of Alzheimer's disease and brain amyloidosis [29]. Our data suggest that in HC plasma samples Aβ peptides could be present mainly in a soluble form, not associated to EVs (the Aβ levels measured in plasma with ELISA assay could come predominantly from free Aβ peptides). On the other hand, in AD the circulating Aβ peptides seem to be widely carried by EV structures that, indeed, appeared to be enriched in Aβ compared to EVs from HC samples. These observations provide further support to the theory that indicates the potential role of EVs in the AD pathological processes as carriers of specific molecules involved in the amyloidogenic pathway.

4. Conclusion

In this work we propose an SPRi-based biosensor for the detection of multiple circulating EVs as biomarkers of Alzheimer's disease that could be used for the identification and monitoring in rehabilitation treatment of the neurodegenerative condition. AD has a complex and not fully understood molecular pathogenesis and a unique and easily accessible marker has not been identified, yet. Our results show the possibility to monitor the progression of the disease by combining different factors that are involved in the pathology through the multiplexing analysis of plasma EVs as complex carriers of multiple disease biomarkers. Indeed, the evaluation of the presence and/or the amount of specific bioactive molecules, such as TSPO, GM1 and Aβ, loaded on the neural EVs, is a valid way to gain a snapshot of the pathological mechanisms that are taking place in the neural tissue, which could be used for the identification of the physio/pathological condition of a subject. We also identify the SPRi intensity CD11b/IB4 ratio as a new possible value that has a significant correlation with the volume of the hippocampus in AD patients. This is an interesting factor that strengthens the hypothesis of using specific populations of circulating EVs (detected according to the commonly used markers for EVs released by each neural cell type) as markers of AD progression, as they could be loaded with altered cargoes during the disease.

The study is not without limitations. The small sample size of the sample and the difference in age between groups makes the study only a pilot investigation. Indeed, AD and HC groups were matched for gender (chi-square analysis, $p = 0.661$) but not for age, with AD older than HC subjects (independent-sample T-Test, $p = 0.0002$, as reported in Table 1). To improve our findings, furthers studies involving more patients with different ATN profiles and syndromal cognitive stages, together with age matched control population, are needed. However, the novelty of the proposed approach resides in the biophotonics-based analysis of the molecular components carried by populations of circulating EVs. Taking advantage of the technological innovation we have confirmed the potentiality of EVs as biomarkers of AD that could enhance the accuracy and the reliability of diagnosis, allowing a proper stratification of patients and potentially providing a powerful tool for the evaluation of the efficacy of new therapeutics in clinical trials and rehabilitative protocols, thus proposing a possible solution to the deep impact that this disease has in the society. To make our findings even more reliable, these EVs properties need a clinical validation through studies involving more patients, also at different stages of the disease, and including patients with other neurological disorders as pathological controls in order to verify the specificity of EV profiling in AD. Compared to a recently proposed platform for the detection of EV-associated amyloid as AD biomarker [30], our work does not focus on a specific protein for the stratification of patients, but proposes a multiplexing approach to the biomarker discovery in AD. The analysis of different populations of circulating EVs could reveal novel correlations previously masked by single-molecule measurements and advance future blood-based clinical management of AD.

Funding sources

This work was supported by Italian Ministry of Health (Ricerca Corrente 2017–2018, IRCCS Fondazione Don Carlo Gnocchi ONLUS).

CRediT authorship contribution statement

Silvia Picciolini: Conceptualization, Data curation, Formal analysis, Visualization, Writing - original draft, Writing - review & editing, Funding acquisition, Investigation, Methodology, Resources. **Alice Gualerzi:** Conceptualization, Data curation, Validation, Writing - review & editing, Methodology. **Cristiano Carlomagno:** Data curation, Formal analysis, Methodology, Software, Writing - review & editing. **Monia Cabinio:** Formal analysis, Investigation, Resources, Software, Visualization, Writing - review & editing.

Stefano Sorrentino: Formal analysis, Investigation, Methodology, Visualization, Writing - review & editing. **Francesca Baglio:** Resources, Supervision, Writing - review & editing. **Marzia Bedoni:** Funding acquisition, Project administration, Resources, Supervision, Validation, Writing - review & editing.

Declaration of Competing Interest

The authors reported no declarations of interest.

Acknowledgements

TEM analysis was carried out in ALEMBIC, an advanced microscopy laboratory established by IRCCS Ospedale San Raffaele and Università Vita-Salute San Raffaele (Milan, Italy).

References

[1] W.H. Organisation, Global Action Plan on the Public Health Response to Dementia 2017 - 2025, Geneva World Heal. Organ, 52, 2017 http://www.who.int/mental_health/neurology/dementia/action_plan_2017_2025/en/.
[2] G.M. McKhann, D.S. Knopman, H. Chertkow, B.T. Hyman, C.R. Jack, C.H. Kawas, W.E. Klunk, W.J. Koroshetz, J.J. Manly, R. Mayeux, R.C. Mohs, J.C. Morris, M.N. Rossor, P. Scheltens, M.C. Carrillo, B. Thies, S. Weintraub, C.H. Phelps, The diagnosis of dementia due to Alzheimer's disease: recommendations from the National Institute on Aging-Alzheimer's Association workgroups on diagnostic guidelines for Alzheimer's disease, Alzheimer's Dement. 7 (2011) 263–269, http://dx.doi.org/10.1016/j.jalz.2011.03.005.
[3] C.R. Jack, H.J. Hampel, S. Universities, M. Cu, R.C. Petersen, A new classification system for AD, independent of cognition A / T / N : An unbiased descriptive classification scheme for Alzheimer disease biomarkers, Neurology 0 (2016) 1–10.
[4] C.R. Jack, D.A. Bennett, K. Blennow, M.C. Carrillo, B. Dunn, S.B. Haeberlein, D.M. Holtzman, W. Jagust, F. Jessen, J. Karlawish, E. Liu, J.L. Molinuevo, T. Montine, C. Phelps, K.P. Rankin, C.C. Rowe, P. Scheltens, E. Siemers, H.M. Snyder, R. Sperling, C. Elliott, E. Masliah, L. Ryan, N. Silverberg, NIA-AA Research Framework: toward a biological definition of Alzheimer's disease, Alzheimer's Dement. 14 (2018) 535–562, http://dx.doi.org/10.1016/j.jalz.2018.02.018.
[5] E. Niemantsverdriet, S. Valckx, M. Bjerke, S. Engelborghs, Alzheimer's disease CSF biomarkers: clinical indications and rational use, Acta Neurol. Belg. 117 (2017) 591–602, http://dx.doi.org/10.1007/s13760-017-0816-5.
[6] H. Hampel, S.E. O'Bryant, J.L. Molinuevo, H. Zetterberg, C.L. Masters, S. Lista, S.J. Kiddle, R. Batrla, K. Blennow, Blood-based biomarkers for Alzheimer disease: mapping the road to the clinic, Nat. Rev. Neurol. 14 (2018) 639–652, http://dx.doi.org/10.1038/s41582-018-0079-7.
[7] A. Badhwar, A.S. Haqqani, Biomarker potential of brain-secreted extracellular vesicles in blood in Alzheimer's disease, Alzheimer's Dement. Diagnosis, Assess. Dis. Monit. 12 (2020) 1–14, http://dx.doi.org/10.1002/dad2.12001.
[8] A.F. Hill, NeuroEVs : characterizing extracellular vesicles generated in the neural domain, by extracellular vesicles and neurodegenerative diseases, J. Neurosci. 39 (2019) 9269–9273, http://dx.doi.org/10.1523/JNEUROSCI.0147-18.2019.
[9] M.B. Dinkins, G. Wang, E. Bieberich, Sphingolipid-enriched extracellular vesicles and alzheimer's disease: a decade of research, J. Alzheimers Dis. 60 (2017) 757–768, http://dx.doi.org/10.3233/JAD-160567.
[10] R. Szatanek, M. Baj-Krzyworzeka, J. Zimoch, M. Lekka, M. Siedlar, J. Baran, The methods of choice for extracellular vesicles (EVs) characterization, Int. J. Mol. Sci. 18 (2017), http://dx.doi.org/10.3390/ijms18061153.
[11] T. Rojalin, B. Phong, H. Koster, R.P. Carney, Nanoplasmonic approaches for sensitive detection and molecular characterization of extracellular vesicles, Front. Chem. 7 (2019), http://dx.doi.org/10.3389/fchem.2019.00279.
[12] E.L. Gool, I. Stojanovic, R.B.M. Schasfoort, A. Sturk, T.G. Van Leeuwen, R. Nieuwland, L.W.M.M. Terstappen, F.A.W. Coumans, Surface plasmon resonance is an analytically sensitive method for antigen profiling of extracellular vesicles, Clin. Chem. 63 (2017) 1633–1641, http://dx.doi.org/10.1373/clinchem.2016.271049.
[13] S. Picciolini, A. Gualerzi, R. Vanna, A. Sguassero, F. Gramatica, M. Bedoni, M. Masserini, C. Morasso, Detection and characterization of different brain-derived subpopulations of plasma exosomes by surface plasmon resonance imaging, Anal. Chem. 90 (2018) 8873–8880, http://dx.doi.org/10.1021/acs.analchem.8b00941.
[14] J. Van Deun, P. Mestdagh, P. Agostinis, Ö. Akay, S. Anand, J. Anckaert, et al., EV-TRACK: transparent reporting and centralizing knowledge in extracellular vesicle research, Nat. Methods 14 (2017) 228–232, http://dx.doi.org/10.1038/nmeth.4185.
[15] J.E. Iglesias, J.C. Augustinack, K. Nguyen, C.M. Player, A. Player, M. Wright, N. Roy, M.P. Frosch, A.C. McKee, L.L. Wald, B. Fischl, K. Van Leemput, A computational atlas of the hippocampal formation using ex vivo, ultra-high resolution MRI: Application to adaptive segmentation of in vivo MRI, Neuroimage 115 (2015) 117–137, http://dx.doi.org/10.1016/j.neuroimage.2015.04.042.
[16] C. Théry, K.W. Witwer, E. Aikawa, M.J. Alcaraz, J.D. Anderson, R. Andriantsitohaina, et al., Minimal information for studies of extracellular vesicles 2018 (MISEV2018): a position statement of the International Society for Extracellular Vesicles and update of the MISEV2014 guidelines, J. Extracell. Vesicles 7 (2018), http://dx.doi.org/10.1080/20013078.2018.1535750.
[17] M. Perrotte, M. Haddad, A. Le Page, E.H. Frost, T. Fulöp, C. Ramassamy, Profile of pathogenic proteins in total circulating extracellular vesicles in mild cognitive impairment and during the progression of Alzheimer's disease, Neurobiol. Aging 86 (2020) 102–111, http://dx.doi.org/10.1016/j.neurobiolaging.2019.10.010.
[18] M. Mustapic, E. Eitan, J.K. Werner, S.T. Berkowitz, M.P. Lazaropoulos, J. Tran, E.J. Goetzl, D. Kapogiannis, Plasma extracellular vesicles enriched for neuronal origin: a potential window into brain pathologic processes, Front. Neurosci. 11 (2017) 1–12, http://dx.doi.org/10.3389/fnins.2017.00278.
[19] E.B. Pasquale, Exosomes expand the sphere of influence of Eph receptors and ephrins, J. Cell Biol. 214 (2016) 5–7, http://dx.doi.org/10.1083/jcb.201606074.
[20] C.N. Winston, H.K. Romero, M. Ellisman, S. Nauss, D.A. Julovich, T. Conger, J.R. Hall, W. Campana, S.E. O'Bryant, C.M. Nievergelt, D.G. Baker, V.B. Risbrough, R.A. Rissman, Assessing neuronal and astrocyte derived exosomes from individuals with mild traumatic brain injury for markers of neurodegeneration and cytotoxic activity, Front. Neurosci. 13 (2019) 1–14, http://dx.doi.org/10.3389/fnins.2019.01005.
[21] E.M. Krämer-Albers, N. Bretz, S. Tenzer, C. Winterstein, W. Möbius, H. Berger, K.A. Nave, H. Schild, J. Trotter, Oligodendrocytes secrete exosomes containing major myelin and stress-protective proteins: trophic support for axons? Proteomics - Clin. Appl. 1 (2007) 1446–1461, http://dx.doi.org/10.1002/prca.200700522.
[22] K.A. Clayton, A.A. Van Enoo, T. Ikezu, Alzheimer's disease: The role of microglia in brain homeostasis and proteopathy, Front. Neurosci. 11 (2017) 1–23, http://dx.doi.org/10.3389/fnins.2017.00680.
[23] F. Agosta, D.D. Libera, E.G. Spinelli, A. Finardi, E. Canu, A. Bergami, L.B. Chiavetto, M. Baronio, G. Comi, G. Martino, M. Matteoli, G. Magnani, C. Verderio, R. Furlan, Myeloid microvesicles in cerebrospinal fluid are associated with myelin damage and neuronal loss in mild cognitive impairment and Alzheimer disease, Ann. Neurol. 76 (2014) 813–825, http://dx.doi.org/10.1002/ana.24235.
[24] A. Katsumoto, H. Takeuchi, K. Takahashi, F. Tanaka, Microglia in Alzheimer's disease: risk factors and inflammation, Front. Neurol. 9 (2018) 1–7, http://dx.doi.org/10.3389/fneur.2018.00978.
[25] M. Cabinio, M. Saresella, F. Piancone, F. LaRosa, I. Marventano, F.R. Guerini, R. Nemni, F. Baglio, M. Clerici, Association between hippocampal shape, neuroinflammation, and cognitive decline in Alzheimer's disease, J. Alzheimers Dis. 66 (2018) 1131–1144, http://dx.doi.org/10.3233/JAD-180250.
[26] E.L. Werry, F.M. Bright, O. Piguet, L.M. Ittner, G.M. Halliday, J.R. Hodges, M.C. Kiernan, C.T. Loy, J.J. Kril, M. Kassiou, Recent developments in TSPO PET imaging as a biomarker of neuroinflammation in neurodegenerative disorders, Int. J. Mol. Sci. 20 (2019) 1–21, http://dx.doi.org/10.3390/ijms20133161.
[27] K. Yuyama, N. Yamamoto, K. Yanagisawa, Accelerated release of exosome-associated GM1 ganglioside (GM1) by endocytic pathway abnormality: another putative pathway for GM1-induced amyloid fibril formation, J. Neurochem. 105 (2008) 217–224, http://dx.doi.org/10.1111/j.1471-4159.2007.05128.x.
[28] F. Li, X.Y. Xie, X.F. Sui, P. Wang, Z. Chen, J.B. Zhang, Profile of pathogenic proteins and MicroRNAs in plasma-derived extracellular vesicles in alzheimer's disease: a pilot study, Neuroscience 432 (2020) 240–246, http://dx.doi.org/10.1016/j.neuroscience.2020.02.044.
[29] V. Pérez-Grijalba, J. Arbizu, J. Romero, E. Prieto, P. Pesini, L. Sarasa, F. Guillen, I. Monleón, I. San-José, P. Martínez-Lage, J. Munuera, I. Hernández, M. Buendía, O. Sotolongo-Grau, M. Alegret, A. Ruiz, L. Tárraga, M. Boada, M. Sarasa, M. Goñi, F. Pujadas, A. Villarejo, A. Frank, J. Peña-Casanova, M. Fernández, G. Piñol, R. Blesa, P. Gil, L.F. Pascual, M. Aguilar, G.B. Frisoni, J. Matias-Guiu, N. Andreasen, C. Antúnez, Plasma Aβ42/40 ratio alone or combined with FDG-PET can accurately predict amyloid-PET positivity: a cross-sectional analysis from the AB255 Study, Alzheimers Res. Ther. 11 (2019) 1–9, http://dx.doi.org/10.1186/s13195-019-0549-1.
[30] C.Z.J. Lim, Y. Zhang, Y. Chen, H. Zhao, M.C. Stephenson, N.R.Y. Ho, Y. Chen, J. Chung, A. Reilhac, T.P. Loh, C.L.H. Chen, H. Shao, Subtyping of circulating exosome-bound amyloid β reflects brain plaque deposition, Nat. Commun. 10 (2019) 1–11, http://dx.doi.org/10.1038/s41467-019-09030-2.